Concentration Levels, Spatial Distribution and Source Identification of PAHs, n-Alkanes, Hopanes and Steranes in Deposited Dust of Mashhad, Iran, and Potential Health Risk Assessment

Mahdad, F., Bakhtiari, A. R., Moeinaddini, M., Charlesworth, S. & Emrani, N

DOI 10.1007/s40710-022-00591-x
ISSN 2198-7491
ESSN 2198-7505

Publisher: Springer

The final publication is available at Springer via http://dx.doi.org/10.1007/s40710-022-00591-x

Concentration Levels, Spatial Distribution and Source Identification of PAHs, *n*-Alkanes, Hopanes and Steranes in Deposited Dust of Mashhad, Iran, and Potential Health Risk Assessment

Faezeh Mahdad, Alireza Riyahi Bakhtiari, Mazaher Moeinaddini, Susanne Charlesworth and Nima Emrani

Abstract
This study investigated the carcinogenic contamination level of deposited dust (DD) on the roof near heating, ventilation, and air conditioning systems (HVAC), which can greatly affect the indoor air quality. Forty samples of roof DD were collected, and organic compounds (16 PAH compounds, 20 *n*-alkane homologs, 8 hopanes, and 6 steranes) were extracted using Soxhlet and analyzed by GC-MS. Source identification of organic compounds was conducted by ring classification, diagnostic ratios, and principal component analysis (PCA) was done. The results showed that the average ± SD of total PAHs, *n*-alkanes, hopanes and steranes in DD were 1356.00 ± 291.45 $\mu g.kg^{-1}$, 3211.65 ± 969.18 $\mu g.g^{-1}$, 146.37 ± 79.45 $\mu g.g^{-1}$ and 469.76 ± 188.25 $\mu g.g^{-1}$, respectively. Also, the highest concentration of organic compounds was measured in the city center, where traffic congestion is expected. Diagnostic ratios of *n*-alkanes results revealed the vehicular emission as dominant source. On the other hand, PCA indicated vehicular and biogenic emission as the primary sources. Sterane and hopane profiles also confirm these results. Moreover, PAHs diagnostic ratios indicated petroleum combustion as the primary source and PCA showed that vehicular emissions, and natural gas and wood combustion were the main factors. The incremental lifetime cancer risk of PAHs was calculated as 8.45×10^{-12} for children and 9.80×10^{-7} for adults, and the imposed risk is considered negligible. Based on the results, diesel and gasoline-powered vehicles are responsible for a significant proportion of the hydrocarbon pollution in Mashhad.

Keywords Source identification · Polycyclic aromatic hydrocarbons · Deposited dust · Molecular markers · Health Risk Assessment

1 Introduction

Since people in urban areas experience many indoor hours, it is crucial to maintain good indoor air quality (Liu et al. 2018). The applied system for heating, ventilation, and air conditioning (HVAC) in a building can considerably alter the quality of indoor air. The HVAC system can influence supplied air quality, and a polluted supply air system can deteriorate indoor air quality (Holopainen et al. 2002). According to (Tringe et al. 2008, HVAC dust could provide an integrated indicator of indoor airborne pollution levels. Several researchers have also looked at the concentrations of heavy metals and PAHs in household dust, as well as their relationships with possible sources (indoor and outdoor) and distribution of particle size (Al-Rajhi et al. 1996; Chattopadhyay et al. 2003; Khedidji et al. 2013; Al Ali et al. 2017; Škrbić et al. 2019; Azimi et al. 2020). The difference in emission sources of PAHs (i.e., traffic emissions, domestic heating, industrial activities, agricultural waste and biomass burnings, and forest fires) should be exposed (Pongpiachan et al. 2017). The chemical profile of particulate PAHs from various sources was of interest to some studies which evaluated vehicle releases (He et al. 2006; Mihankhah et al. 2020; Zhen et al. 2020), motorcycle exhausts (Pham et al. 2013; Davoudi et al. 2021), shipping emissions (Pongpiachan et al. 2017), and various types of biomass burning (Sanchis et al. 2014; Du et al. 2020; Nowakowski et al. 2022; Ofori et al. 2021; Yang et al. 2021; Zhang et al. 2021). PAH concentrations in the air were assessed individually at indoor and outdoor sites, and higher concentrations of PAHs were detected in indoor samples than in outdoor ones (Pandit et al. 2001; Delgado-Saborit et al. 2011) evaluated the presence of PAHs in indoor and outdoor environments and their total carcinogenic potential. PAHs are hydrophobic, carcinogenic, lipophilic, and persistent to degradation. They are also known among the most toxic organic pollutants. PAHs can cause severe detrimental health effects as they are carcinogenic to humans (Mihankhah et al. 2020; Wu et al. 2021). The results have shown that indoor PAH concentrations are higher than the outdoor ones at buildings close to traffic (Delgado-Saborit et al. 2011). Wintertime PAH concentrations in indoor and outdoor air samples in a large dormitory for students in Algiers revealed higher indoor PAH levels compared to outdoor levels, posing a significant health risk (Khedidji et al. 2013).

Particulate matter (PM) is a significant air pollutant that degrades air quality in arid and semi-arid areas (Soleimani et al. 2016). Residential exposure to indoor contaminants has been measured using deposited dust (DD). Environmental and seasonal influences, ventilation and air filtration, resident habits, and indoor and outdoor pollutant sources all affect the composition of indoor dust (Maertens et al. 2004). Heating, ventilation, and HVAC systems substantially affect indoor air quality, and most buildings in the Middle East have HVAC on the roof. By providing an empirically based, post-hoc exposure metric at the household scale, DD on the roof can provide a valuable means of refining exposure estimates in such contexts. Furthermore, the particle size of DD near the ground surface is smaller than that near the top of the roof (Kramer et al. 2020). It comprises clumps of material that come pri-

marily from outside sources, such as aerosol and soil deposition, rather than from domestic operations (Sajn 2005).

Being absorbed onto PM is a possibility for PAHs in the atmosphere (Wu et al. 2021) which makes the absorbed PM more easily transportable (Ghanavati et al. 2019; Wu et al. 2021). Chemical characterization of deposited urban dust is similar to a significant portion of the atmospheric aerosol in many aspects. Also, fugitive dust moves in the urban environment frequently by resuspension and deposition. Therefore, urban dust characterization can assess environmental quality (Mihankhah et al. 2020; Wu et al. 2021). Several studies worldwide have looked into persistent organic pollutants (POPs) like PAHs that belong to PM and DD (Omar et al. 2007; Dong and Lee 2009; Mostafa et al. 2009; Al Ali et al. 2017; Škrbić et al. 2019), with high levels of PM and DD identified in some of Iran's major cities (Saeedi et al. 2012; Soltani et al. 2015; Keshavarzi et al. 2018, 2020; Azimi et al. 2018; Ghanavati et al. 2019). PAHs, *n*-alkanes, *n*-alkanoic acid, hopanes, steranes, and other compounds make up the organic fraction of DD. Some of these compounds, such as PAHs, hopanes and steranes, are persistent and potentially harmful, posing a significant health risk as they can cause mutagenic and carcinogenic effects (Liu et al. 2015). These various organic compounds, on the other hand, can be used as a source recognition and health risk assessment marker (Javed et al. 2019).

Molecular marker analysis may also be used to classify organic matter origins, allowing for comparing identified sources and observed atmospheric organic compound mixtures (Omar et al. 2007; Mostafa et al. 2009; Zhang et al. 2017). PAHs and other organic pollutants may be adsorbed onto PM (Najmeddin et al. 2018; Ghanavati et al. 2019; Javed et al. 2019). PAH compounds are biodegradable and may not be stable in the environment after release. Other markers, in addition to PAHs, could aid in the identification of particle sources. As a result of their low reactivity and volatility, *n*-alkanes are solid indicators for air transport and particle sources (Omar et al. 2007; Zhang et al. 2017). Photochemical and microbial degradation can hardly influence other petroleum indicators, such as hopanes and steranes, because they are complex cyclic molecules (Alves et al. 2018). As a result, these markers will produce precise source information critical to environmental forensics investigations to research hydrocarbon fate and activity in the environment (Omar et al. 2007; Mostafa et al. 2009).

Comparing the diagnostic ratios (DRs) of commonly occurring organic pollutant pairs can lead to the characterization of organic pollutant source variation (Ravindra et al. 2008). Hence, there was a broad application of molecular DRs to qualitatively define the sources of air pollutants (Omar et al. 2007; Bahry et al. 2009; Azimi et al. 2018). However, these ratios should be used with caution due to the variations in pollution sources and the decomposition of most organic-based contaminants within the atmosphere due to their reactions with the oxidants present in the atmosphere (Zakaria et al. 2000; Moeinaddini et al. 2014a).

The DD could be transported indoors in the Middle East by HVAC from the roof top. Because of the importance of DD on the roof, as noted previously, a source study and risk assessment of DD were needed. The project aimed to measure the concentration and spatial distribution of PAHs, *n*-alkanes, hopanes, and steranes present in DD, as well as pollution levels, source identification, and an assessment of the potential cancer risk related to PAH exposure from DD through dermal contact, ingestion, and inhalation.

2 Materials and Methods

2.1 Study Area

Mashhad (Latitude 35°59' N to 37°04' N, Longitude 58°22' E to 60°07'E) is the capital of Khorasan Razavi Province in Iran's northeast. It is located at an elevation of 985 m above sea level and has a population of over three million (Fig. 1). The city has experienced rapid growth in recent decades, owing to its economic, social, and religious attractions (Azari and Arintono 2012). It hosts 20 tourism events each year. Mashhad has public transportation, including a subway and a bus rapid transit system (BRT) (Azari and Arintono 2012).

2.2 Sampling and Extraction Methods

Forty DD samples were collected in September 2018 from building roofs in different urban land uses (approximately 3–4 m above ground level) (Fig. 1) at five replicates. The sampling was carried out in the summer, when not only is the temperature the highest and the use of HVAC is the highest, but also the frequency of dust storms is higher than in other seasons (Azimi et al. 2018; Najmeddin and Keshavarzi 2019). The samples were obtained by sweeping 1 m^2 area of the building roof and preserving them in aluminum foil in a zip bag for transport to the laboratory (Wang et al. 2011; Jordanova et al. 2012).

DD samples were dried at room temperature for 24 h, sieved with a 1-mm stainless steel sieve to remove large materials, and placed in a refrigerator at − 4 °C for analysis (Dong and Lee 2009; Škrbić et al. 2019). After that, the samples were freeze-dried for 72 h, and 5 g samples were prepared to extract organic compounds. For quality control (QC), the PAH surrogate internal standard mixture (200 µg kg^{-1} each of naphthalene-d_8, anthracene-d_{10}, perylene-d_{12} and chrysene-d_{12}) was added to the samples. Before analysis, about 5 g of each freeze-dried sample was spiked with 100 µL of *n*-alkanes surrogate internal standard

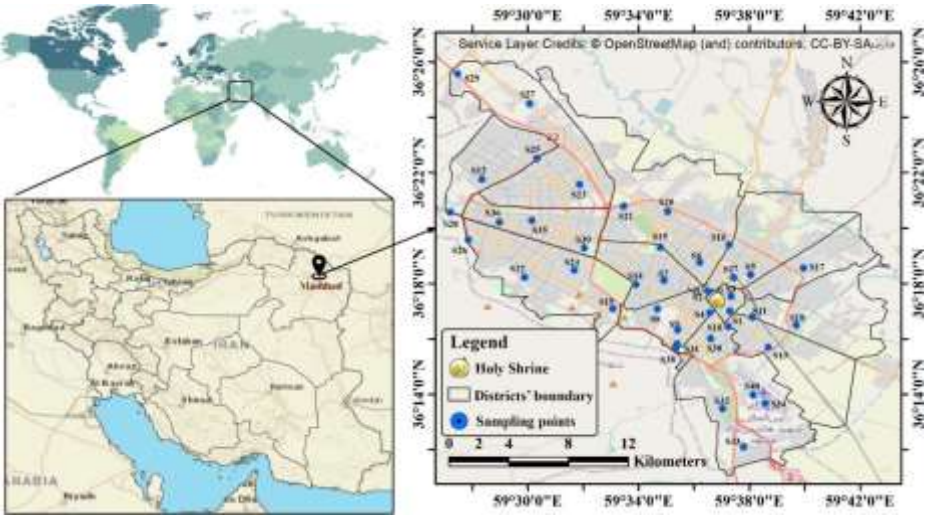

Fig. 1 Study area and sampling site locations in the city of Mashhad, Northeastern Iran

(5 µg g^{-1} of n-dodecane-d_{26}) for aliphatic compounds (*n*-alkanes, hopanes, and steranes). The extraction and fractionation procedure was based on Zakaria et al. (2000) Soxhlet process, which used 100 mL of dichloromethane for 12 h. In summary, this process involves two steps of silica gel chromatography followed by gas chromatography-mass spectrometry analysis of the analytes (GC-MS). Glassware was rinsed with methanol, acetone, and hexane to prevent any contamination. Then, it was heated under a 60 °C temperature for two hours. The external standard solutions of targeted petroleum hydrocarbons were procured from the Sigma Chemical Company. The following 16 PAHs were analyzed: naphthalene (Nap), acenaphthylene (Acy), acenaphthene (Ace), fluorine (Flo), phenanthrene (Phe), anthracene (Ant), fluoranthene (Flt), pyrene (Pyr), benzo(a) anthracene (BaA), chrysene (Chr), benzo(b)fluoranthene (BbF), benzo[k]fluoranthene (BkF), benzo(a)pyrene (BaP), dibenzo[a,h]anthracene (DahA), indeno [1,2,3-cd] pyrene (InP) and benzo[ghi]perylene (BghiP).

Gas chromatograph-mass spectrometer (GC-MS) analyses were performed using GC-7890 A with quadrupole MS-5975 C, Agilent Technologies (PaloAlto, CA, USA). Helium was used as the carrier gas. Sample peak results were detected by comparing the sample results with the retention time of the authentic standard run on the same day con- firmed by GC-MS. In the alkane fraction of samples, biogenic hopanes and diagenetically modified tri- and tetra-cyclic terpanes, hopanes, and steranes were quantified. The single ion monitoring (SIM) mode was used to identify petroleum biomarkers: m/z 191 for tri- and tetracyclic terpane and hopane, m/z 217 for ααα-steranes and m/z 218 for αββ-steranes (Rogge et al. 1993b). The retention times of *n*-alkanes were compared to known standards of *n*-alkanes ranging from n-C_{14} to n-C_{32} to identify them.

2.3 Quality Assurance and Control(QA/QC)

A field blank, a spiked blank, a procedural blank, and a matrix spiked sample were used for each sample (Zakaria et al. 2000; Bakhtiari et al. 2009). About 200 µL of the above-mentioned surrogate internal standard, containing 5 ppm of a mixture of naphthalene-d_8, acenaphthene-d_{10}, phenanthrene-d_{10}, chrysene-d_{12}, and perylene-d_4, was spiked to determine the recovery of the target PAHs. Deuterated *n*-alkanes spiked in each sample were used to estimate the losses of all compounds during sample processing. The average recovery for PAHs ranged between 87% and 104%, *n*-alkanes ranged between 81% and 94%, while for hopanes and steranes it varied from 86 to 101%. Thus, the reported PAHs, *n*-alkanes, and biomarker concentrations for recovery were not corrected (Zheng et al. 2020). The method detection limit (MDL) of hydrocarbons were defined as three times the standard deviation of the blank values. The MDL was calculated based on the standard deviation of the five replicates and the value varied between 0.84 and 2.39 µg kg^{-1} (mean 1.51 µg kg^{-1}) for PAHs, between 1.84 and 3.66 µg g^{-1} (mean 2.72 µg g^{-1}) for *n*-alkanes, 1.34 and 3.19 µg g^{-1} (mean 2.29 µg g^{-1}) for hopanes, and 2.04 and 3.17 ng g^{-1} (mean 2.87 ng g^{-1}) for steranes. Concentrations lower than MDLs were defined as non-detected (N.D.). All concentrations were calculated on a dry weight basis.

2.4 Organic Compounds Source Identification

In this research, widely used DRs for PAH, hopane, sterane, and *n*-alkane indices were measured and compared to the literature to get an initial implication of the organic aerosol emission sources (Omar et al. 2007; Mostafa et al. 2009; Javed et al. 2019). DRs have been effectively used as indicators of PAH sources by various studies (Ravindra et al. 2008; Dong and Lee 2009; Wang et al. 2011; Al Ali et al. 2017; Mon et al. 2020) by considering the relative thermodynamic stability of different parent PAHs and the characteristics of different sources (Bian et al. 2016). The methods used to determine these ratios and indices are presented by Bakhtiari et al. (2011) and Yadav et al. (2013). To find potential PAH sources, DRs for Flt/(Flt + Pyr), BaA/(BaA+ Chr) and InP/(InP+ BghiP) were used. An Flt/Flt + Pyr ratio of less than 0.4 indicates mostly petrogenic sources, 0.4–0.5 indicates fossil fuel combustion, and greater than 0.5 indicates coal and biomass combustion. If the BaA/BaA+ Chr ratio is less than 0.2, it indicates petroleum evaporation, between 0.2 and 0.35 it indicates coal combustion, and greater than 0.35 vehicular emission or combustion (Yunker et al. 2002; Liu et al. 2009). A ratio of InP/InP+ BghiP of less than 0.2 implies gasoline source, 0.2–0.5 petroleum combustion, and > 0.5 combustion of coal or biomass (Yunker et al. 2002).

The carbon numbers of *n*-alkanes, as measured by a carbon preference index (CPI), the percentage of wax (WNA%), and the ratio of unresolved components to resolved components in gas chromatograms (U:R) have all been used in the literature to identify petrogenic (evaporation or combustion) or biogenic sources of *n*-alkanes (Moeinaddini et al. 2014b). The CPI is defined as the ratio of the total concentration of odd carbon number homologues in the sample to the total concentration of even carbon number homologues (Andreou et al. 2008; Duan et al. 2010; Zhang et al. 2017). CPI values are used to compare the contribution of vehicular and human activities to biological sources (Ravindra et al. 2008; Moeinaddini et al. 2014a), with values close to 1 indicating vehicle emissions and other human activities, and values > 3 indicating a predominant origin from biological materials. The WNA% value (WNA= C_n-[(C_{n+1}+C_{n-1})/2], where n is the odd carbon congener, WNA%=($\sum$WNA/$\sum$*n*-alkanes)×100) is calculated for odd carbon number homologues, and it is used to indicate biogenic as opposed to petrogenic sources (Rogge et al. 1993a; Omar et al. 2007; Andreou et al. 2008; Zhang et al. 2017; Javed et al. 2019).

The U:R was applied to determine the pollution level caused by the residues of petroleum, and it can also be used to differentiate between the sources, i.e., biomass and fossil fuel combustion (Rogge et al. 1993a; Mostafa et al. 2009; Moeinaddini et al. 2014a; Shirneshan et al. 2017).

Hopanes, as shown in Supplementary Material (SM) Table SM1, are a series of 17α (H), 21β (H) compounds used in this analysis (C_{27} to C_{34}). To characterize petroleum inputs, several geochemical ratios derived from hopane biomarkers were used (Shirneshan et al. 2017). The following ratios were used to analyze hopane distribution patterns further:

- $T_s/(T_s+T_m)$ (ratio of 17α-22,29,30-trisnorhopane relative to 17α-22,29,30-trisnorhopane+ 18α-22,29,30 trisnorhopane),
- C_{29}/C_{30} (ratio of 17α,21β(H)-30norhopane to 17α,21β(H)-hopanes),
- $C_{31}HS/C_{31}H$(S + R) (homehopane index).
- $C_{32}HS/C_{32}H$(S + R) (bishomohopane index).

- $SC_{31}\_C_{35}/C_{30}$ (ratio of sum 17α,21β(H)-C_{31} homohopane to 17α,21β(H)-C_{35} homohopane relative to 17α,21β(H)-hopane),
- C_{28} αββ/(C_{27}αβα + C_{29}αββ) and.
- C_{29} αββ/(C_{27} αββ + C_{28} αββ).

Besides that, PCA was applied to find the PAH and *n*-alkane sources (SPSS version 20.0 for Windows, SPSS Inc.). The Kaiser-Meyer-Olkin (KMO) and Bartlett's tests were also used to assess the suitability of the dataset concerning the PCA; for KMO values of more than 0.6, the data was considered suitable (Ravindra et al. 2008; Moeinaddini et al. 2014a; Škrbić et al. 2021). The PCA of PAHs and *n*-alkanes were conducted separately based on the KMO test results. The varimax rotation method was used. The principal components were chosen where eigenvalues had more than 1. The representative species of the factor were PAHs and n-alkanes with a factor loading of >0.5 (Ravindra et al. 2008; Wang et al. 2011).

2.5 Cancer Risk Assessment of PAHs

The toxic equivalency factor (TEF) of the PAHs was assessed to calculate their carcinogenic potential. The TEF value of Benzo[a]pyrene (BaP) was set to 1 as the reference chemical, and the TEF values of other PAHs were calculated against BaP (Nisbet and Lagoy 1992; Kozliak and Paca 2012; Škrbić et al. 2019). Total Equivalency Factors (TEFs) should be

Table 1 Concentration, statistical parameters, and toxicity aspects (TEF) of investigating PAHs in the deposited dust of Mashhad based on literature review

Compound	No. of rings	TEF	Mean	Min	Max	Median	Std. Dev	Unit
Nap	2	0.001	42.15	60.65	60.65	42.62	8.34	μg/kg
Acy	3	0.001	26.11	42.72	42.72	24.58	6.65	μg/kg
Ace	3	0.001	27.81	44.84	44.84	27.24	6.91	μg/kg
Flo	3	0.001	71.47	102.99	102.99	71.14	12.30	μg/kg
Phe	3	0.001	123.02	170.89	153.39	123.45	23.53	μg/kg
Ant	3	0.01	68.40	118.15	100.65	65.83	15.74	μg/kg
Flt	4	0.001	145.32	212.09	127.09	143.43	31.58	μg/kg
Pyr	4	0.001	163.46	242.14	157.14	158.09	40.36	μg/kg
BaA	4	0.1	117.44	247.86	282.86	121.70	50.98	μg/kg
Chry	4	0.01	100.96	215.80	230.8	91.54	42.29	μg/kg
BbF	5	0.1	85.10	146.48	166.48	84.91	31.24	μg/kg
BkF	5	0.1	83.95	127.29	147.29	84.13	22.69	μg/kg
BaP	5	1	43.81	105.13	105.13	45.00	23.34	μg/kg
DahA	5	1	59.86	103.64	176.33	55.89	13.53	μg/kg
InP	6	0.1	65.02	141.33	128.64	59.82	27.77	μg/kg
BghiP	6	0.01	132.11	251.81	286.81	115.10	44.05	μg/kg
∑16PAHs			1356	1955.75	1955.75	1361.10	291.45	μg/kg
2–3 rings			26.85	31.55	445.53	26.49	2.52	μg/kg
4 rings			38.75	44.61	720.83	38.50	2.60	μg/kg
5–6 rings			34.39	39.12	872.12	34.93	2.78	μg/kg
TEQ			147.08	252.21	252.94	153.05	48.78	μg/kg-BaPeq
ComPAHs/∑PAHs			0.54	0.60	0.6	0.55	0.03	

compared to those of BaP, the most toxic member of the PAH family, to measure the carcinogenicity of individual PAHs (BaP_{eq}). (Nisbet and Lagoy 1992). TEFs were added to each PAH compound, and the toxic equivalent concentration (TEQ) was determined by adding each PAH concentration and its TEF using Eq. (1):

$$TEQs = \sum C_i \times TEF_i \quad (1)$$

where C_i is the PAH_i concentration and TEF_i is the PAH_i toxic equivalency factor. Table 1 presents the TEF values for all PAHs based on Malcolm and Dobson (1994) and Nisbet and Lagoy (1992). The incremental lifetime cancer risk (ILCR) was determined using standard USEPA models to calculate the exposure risk of PAHs (Martuzevicius et al. 2011; Ma et al. 2017). Equations (2)-(4) were used to measure the ILCRs of ingestion, dermal touch, and inhalation:

$$ILCRs_{Ingestion} = \frac{CS \times \left(CSF_{ingestion} \times \sqrt[3]{\frac{BW}{70}}\right) \times IR_{ingestion} \times EF \times ED}{BW \times AT \times 10^6} \quad (2)$$

$$ILCRs_{Dermal} = \frac{CS \times \left(CSF_{Dermal} \times \sqrt[3]{\frac{BW}{70}}\right) \times SA \times AF \times ABS \times EF \times ED}{BW \times AT \times 10^6} \quad (3)$$

$$ILCRs_{Inhalation} = \frac{CS \times \left(CSF_{inhalation} \times \sqrt[3]{\frac{BW}{70}}\right) \times IR_{inhalation} \times EF \times ED}{BW \times AT \times PEF} \quad (4)$$

$$CarcinogenicRisk = ILCR_{Ingestion} + ILCR_{Dermal} + ILCR_{Inhalation} \quad (5)$$

where CS is the sum of the transformed PAHs levels calculated using BaP's toxic equivalents; AF is the skin adherence factor; SA is Dermal exposure area; EF presents exposure frequency; ED is exposure duration; BW is body weight; AT is average life span; ABS is dermal adsorption fraction; $IR_{inhalation}$ is inhalation rate and PEF is Particle emission factor. The BaP carcinogenic factors for intake, exposure, and inhalation are denoted by $CSF_{Ingestion}$, CSF_{Dermal}, and $CSF_{Inhalation}$, respectively. Table SM2 presents additional infor- mation about these parameters.

3 Results and Discussion

3.1 Spatial Distribution and Source Identification of *n*-Alkanes

Figure 2 illustrates the spatial distribution of *n*-alkanes (*n*-C_{14} - *n*-C_{33}) concentration. The highest concentrations ranged from 2131.3 ± 969.18 μg g^{-1} to 5964.6 ± 969.18 μg g^{-1}, with an overall mean of all tests equal to 3159.1 ± 969.18 μg g^{-1}. S1 (6562.0 ± 969.18 μg g^{-1}), S2

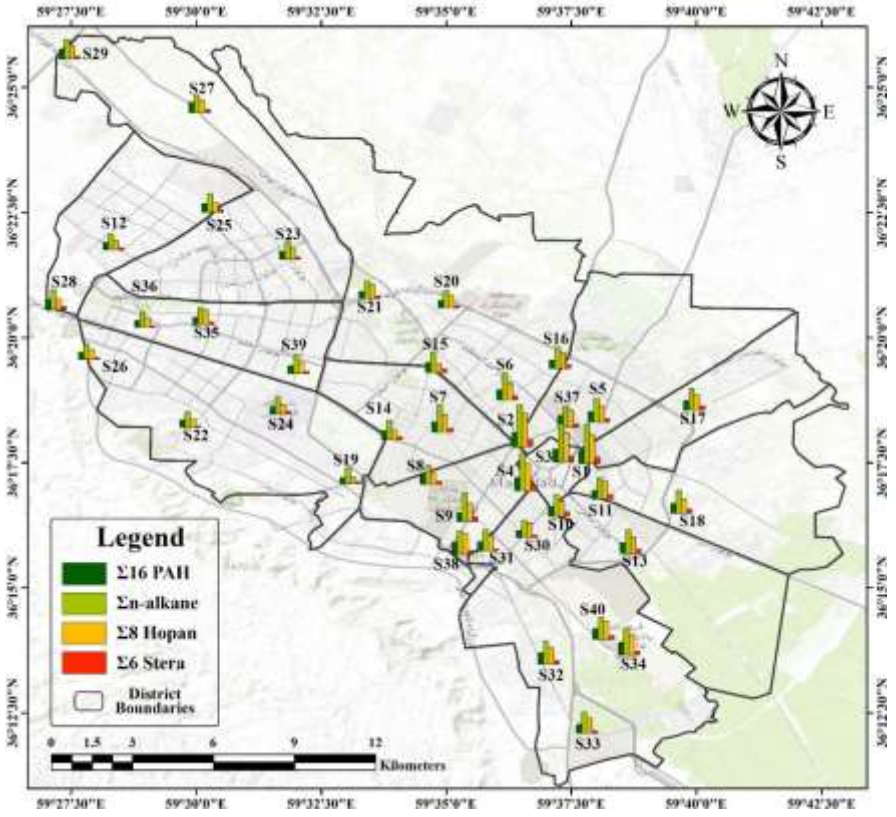

Fig. 2 Distribution of ∑16 PAHs (μg kg^{-1}), ∑20 *n*-alkanes (μg g^{-1}), ∑8 hopanes (μg g^{-1}) and ∑6 steranes (μg g^{-1}) in depositer dust samples of Mashhad, Iran

(5964.6 ± 969.18 μg g^{-1}), S3 (5485.7 ± 969.18 μg g^{-1}) and S4 (5286.3 ± 969.18 μg g^{-1}) had the highest concentrations (Fig. 2). These sites were in the city's core, near the holy shrine, and were highly trafficked. S9 has a concentration of 4004.56 ± 969.18 μg g^{-1} and is located near petrol and car service stations, making it relatively polluted due to the heavy traffic load. On the other hand, the residential area (S26) had the lowest *n*-alkanes concentration (2131.28 ± 969.18) μg g^{-1}). The DD from Mashhad has lower *n*-alkanes concentrations than street dust from other cities, such as Portugal (197–9982 μg g^{-1}; Alves et al. 2018), Malaysia (7360 μg g^{-1}; Omar et al. 2007) and Singapore (3760 μg g^{-1}; Zhang et al. 2017).

Table SM3 shows the DRs results, including the CPI, WNA%, U:R ratio, and Pr:Ph. The CPI values indicated that petroleum residues derived from vehicular emissions are the chief source of *n*-alkanes in most sampling sites, whereas higher plant waxes are found in a few sites. The lower CPI values (0.84–1.52) back up these findings (Table SM3) (Omar et al. 2007; Bakhtiari et al. 2011). The majority of sites were close to 1, but S8, S14 and S28 were all > 1 (1.52, 1.41, and 1.36, respectively). S8 is near Alandasht (10 ha), S14 is near Malek-Abad orchard (> 50 ha), and S28 is located on the Shandiz-Torqaba road, where many orchards are located. Higher values for the CPI demonstrate *n*-alkanes derived from

plant waxes and are characteristic of well-protected biomarker signals (Mostafa et al. 2009; Thomas et al. 2021).

GC–MS traces of hydrocarbons or total extracts detected in urban DD usually consist of large unresolved complex mixtures (UCM) composed of branched and cyclic (petro- leum) compounds (Fig. SM1). The majority of these hydrocarbons come from the use of fossil fuels, which comprise the main components of both diesel and auto engine exhaust (Rogge et al. 1993b; Simoneit 1984, 1985). Biogenic hydrocarbons derived from higher plants exhibit no UCM (Simoneit and Mazurek 1982). A UCM in the range of *n*-C_{20}–*n*-C_{33} alkanes was observed in all samples, indicating samples polluted by biodegraded petroleum residues (Andreou et al. 2008; Mostafa et al. 2009).

The U:R ratio (i.e., the UCM ratio to plant wax *n*-alkanes) can be used to determine pollution from petroleum product combustion of vehicular sources since the UCM is primarily formed by fossil fuel applications (Omar et al. 2007; Jafarabadi et al. 2018, 2019). Besides that, the U:R ratio was used as a contaminant input diagnostic criterion, where values› 2 show significant pollution by petroleum products (Jafarabadi et al. 2019). The U:R ratios for all samples were greater than 2, indicating petrogenic sources. This was in line with the UCM profile and low CPI values (Table SM3). The U:R ratios were applied to express the extent of vehicular exhaust contribution to street dust hydrocarbons (Simoneit 1999) which increases as vehicular exhaust contribution increases. The U:R ratio is much less than that

Table 2 The results of principal component analysis (PCA) for *n*-alkanes

	n-alkane Factor	
	1	2
n-C_{14}	***0.51***[a]	0.09
n-C_{15}	***0.53***	0.12
n-C_{16}	***0.62***	0.22
n-C_{17}	***0.77***	0.14
n-C_{18}	***0.81***	0.15
n-C_{19}	***0.84***	0.32
n-C_{20}	***0.79***	0.39
n-C_{21}	***0.77***	0.44
n-C_{22}	***0.72***	0.48
n-C_{23}	***0.66***	***0.54***
n-C_{24}	0.49	***0.66***
n-C_{25}	0.36	***0.72***
n-C_{26}	0.48	***0.55***
n-C_{27}	0.47	***0.72***
n-C_{28}	0.43	***0.66***
n-C_{29}	0.07	***0.57***
n-C_{30}	0.14	***0.79***
n-C_{31}	0.15	***0.70***
n-C_{32}	0.05	***0.83***
n-C^{33}	0.26	***0.60***
Pr	***0.68***	0.03
Ph	***0.69***	0.06

[a] Values in bold/italics are for factor loading values> 0.5 and indicate important factors for each component

estimated in road dust in Athens, Greece (Andreou et al. 2008) but much higher for street dust in Egypt (Mostafa et al. 2009). A comparison of *n*-alkanes DRs in DD with PM and street dust of other cities worldwide are given in Table SM4.

The most abundant petroleum isoprenoids are pristane (2,6,10,14-tetramethylpentadecane, C_{19} isoprenoid) and phytane (2,6,10,14-tetramethylhexadecane, C_{20} isoprenoid) (Shirneshan et al. 2017). They can be found in diesel fuel, lubricating oil, from gasoline and diesel engine exhaust (Simoneit 1984, 1985). The presence of pristane and phytane in the UCM, and also the Pr:Ph ratio of 0.18 to 0.76 implied petroleum residue pollution (Omar et al. 2007).

Figure SM2 and Table 2 illustrate the PCA results, with two principal components representing three potential sources listed. High loading values for low to medium molecular weight ($\leq nC_{24}$) *n*-alkanes with the presence of Pr and Ph were found in the first factor (48.63% of variance), indicating contribution from fossil fuel combustion, especially vehicular emissions (Duan et al. 2010; Moeinaddini et al. 2014a). The second factor, with 36.57% of the total variance, is associated with longer chain *n*-alkanes ($> nC_{24}$). As a result, it was concluded that the significant sources of *n*-alkanes in the DD are most likely vehicle exhaust and fuel combustion.

3.2 Spatial Distribution and Source Identification of Hopanes and Steranes

Mass fragmentograms of m/z 191 (hopanes) and m/z 217–218 (steranes) for samples were presented in Fig. SM3. The mean concentration of hopanes was 2209.8 ± 79.45 μg g^{-1} dw. The highest hopane concentrations were observed at S2, S1, S3 and, S4, equal to 4860.1 ± 79.45 μg g^{-1} dw, 4241.0 ± 79.45 μg g^{-1} dw, 4193.9 ± 79.45 μg g^{-1} dw, and 3940.6 ± 79.45 μg g^{-1} dw, respectively. These stations are in the city center, close to the holy shrine, and have heavy traffic and air pollution, including the underpass of the holy shrine (Imam Reza). S38 (3120.50 μg g^{-1} dw) is located at the passenger bus terminal, where heavy bus traffic leads to high hopane concentrations. On the other hand, the lowest concentration was found in the residential area at S19 (979.34 ± 79.45 μg g^{-1} dw). Hopane levels in this study were relatively lower than the ones measured in street dust from Portugal (2706 μg g^{-1}; Alves et al. 2018) and Anzali, Iran (5225.58 μg g^{-1}; Azimi et al. 2018), but higher than those in Singapore (153.47 μg g^{-1}; Zhang et al. 2017) and Malaysia (389 μg g^{-1}; Omar et al. 2007).

In this study, the ααα- and αββ-steranes ranging from C_{27} to C_{29} were analyzed to be 20 S and 20R isomers in the DD (Omar et al. 2007). The mean concentration of steranes was 469.79 ± 188.25 μg g^{-1} dw. The highest concentrations were found in the same locations with the hopanes (S2, S3, S1, and S4). On the other hand, the lowest concentration of steranes was in residential areas at S19 (185.24 ± 188.25 μg g^{-1} dw) and S22 (193.25 ± 188.25 μg g^{-1} dw). Sterane levels of street dust samples in this study were relatively higher than the ones measured in Singapore (30.18 μg g^{-1}; Zhang et al. 2017), Malaysia (50 μg g^{-1}; Omar et al. 2007) and Anzali, Iran (250.98 μg g^{-1}; Azimi et al. 2018). The comparison of hopane and sterane DRs in the present study with other cities worldwide is shown in Table SM5.

Petroleum biomarkers such as diasteranes, steranes and hopanes are molecular biomarkers found in crude oils used to monitor petrogenic-related inputs into the environment, including street dust and airborne PM (Rogge et al. 1993b; El Haddad et al. 2009). Hopanes

and steranes are released in the most significant amounts by gasoline and diesel-fueled vehicles (Mostafa et al. 2009; Alves et al. 2017).

The $T_s/(T_s+T_m)$ ratio was calculated in this study using Han et al. (2015) find- ings for vehicle exhaust particles (0.53–0.61) (Han et al. 2015). The homopane index, $C_{31}\alpha\beta S/(C_{31}\alpha\beta S + C_{31}\alpha\beta R)$, is one of the most common indices used (Omar et al. 2007; Alves et al. 2017); the values in this study were between 0.4 and 0.77 (Table SM3), and for the bishomohopane index $C_{32}[S/(S+R)]$ ratios were 0.34 to 0.72 (Table SM3) (Alves et al. 2017; Han et al. 2015) found that the $C_{32}[S/(S + R)]$ ratios for each form of coal smoke were lower (< 0.44) than those for vehicle exhausts (0.52–0.64Rogge et al. (1993b) recorded similar ratios for gasoline (0.57) and diesel exhaust (0.59), which are consistent with the findings of this study. Furthermore, the C_{31}-C_{35}/C_{30} ratio provides additional information for determining the source of airborne particles (Zakaria et al. 2002; Bahry et al. 2009; Alves et al. 2017; Zhang et al. 2017). Except for high-rank (anthracite) coal, $C_{29}\alpha\beta/C_{30}\alpha\beta$ ratios > 1 were recorded for both residential and industrial coal burning, while vehicle exhausts had values of 0.42–0.59 (Han et al. 2015). These results, therefore, indicate that traffic-related emissions are the primary sources of hopanes and steranes. The mixture of lubricating oil from automobiles and street dust and soot particles, and their subsequent re-suspension, according to Bahry et al. (2009), is likely to be a significant source of atmospheric hopanes.

3.3 Spatial Distribution and Source Identification of PAHs

Sixteen PAH compounds introduced by USEPA were present and detected in all samples; statistical analysis of the results is presented in Fig. 2. The mean ∑PAHs content was 945.80 ± 291.45 μg kg^{-1} dw. The highest concentrations were observed in S2, S1, S3, and S4 (1580.79 ± 291.45, 1457.25 ± 291.45, 1409.25 ± 291.45, and 1389.51 ± 291.45 μg kg^{-1} dw, respectively). These sampling sites are located in the city center near the holy shrine and are surrounded by congested roads (Fig. 1).

One of the key explanations for the high concentrations of PAHs observed at some sampling stations is likely due to the limited dispersion of pollutants from their primary source (Wang et al. 2011; Škrbić et al. 2017, 2021). S38, for example, is near a bus terminal and has a relatively high concentration of 1008.24 μg kg^{-1} dw, which may be due to engine oil and diesel leakage. On the other hand, S19 had the lowest concentration (464.26 ± 291.45 μg kg^{-1} dw), even though it is a lightly trafficked residential area with no industrial activi- ties. Maliszewska-Kordybach (1996) classified the levels of contamination into four classes according to PAH concentrations: (1) not contaminated (< 200 μg kg^{-1}); (2) slightly contaminated (200–600 μg kg^{-1}); (3) contaminated (600–1000 μg kg^{-1}), and (4) heavily contaminated (> 1000 μg kg^{-1}).

These categories imply that most samples were contaminated (55%) or slightly contaminated (32.5%). As shown in Table SM4, results also show that the ∑16PAH concentrations were lower than those found in street dust from Mashhad (2183.5 μg kg^{-1} dw ; Najmeddin et al. 2018), and other Iranian cities, including Bushehr (1116.2 μg kg^{-1} dw; Keshavarzi et al. 2020), Isfahan (1074.6 μg kg^{-1} dw; Soltani et al. 2015), and Ahvaz (1031.5 μg kg^{-1} dw; Najmeddin and Keshavarzi 2019). Compared with other cities in the world, ∑16PAH concentration was lower than the analyzed deposited street dust samples in China (Jiang et al. 2014), Japan (Takada et al. 1991), UK (Lorenzi et al. 2011), Egypt (Hassanien and Abdel-Latif 2008), and Korea (Dong and Lee 2009) (Table SM6). It can be concluded that due to

the lack of impact of traffic, i.e., the effect of tire particles, eroded asphalt, lubricating oil leakage and fossil fuels, the concentration of compounds in DD is lower than that of street dust in these cities. However, according to Table SM6, the mean concentration of ∑16PAHs was slightly higher or in the same range as some of those obtained from street dusts in tropical and dry areas (Hassanien and Abdel-Latif 2008; Rastegari Mehr et al. 2016; Keshavarzi et al. 2018; Abbasnejad et al. 2019). The observed differences in the dust–bounded PAH concentrations among these areas could be associated with the economical level, industrial structure, traffic density, population, precipitation, meteorological condition, and the particle size of dust samples (Hussain et al. 2015; Konstantinova et al. 2020).

As shown in Fig. 3a, PAHs were classified into three classes depending on the number of aromatic rings: 2–3, 4, and 5–6, with the percentages of rings being as: 4 ring (33.6– 44.9%, mean 38.8%), 5–6 ring (27.3–39.1%, mean 34.4%) and 2–3 ring (22.3–31.6%, mean 26.89%) (Fig. 3a). The relative minor proportion of lower molecular weight PAHs (2–3 rings) such as naphthalene, acenaphthylene, acenaphthene and fluorine could have its roots in high sensitivity to oxidation through weathering and high solubility in aqueous environ- ments (Omar et al. 2002; Marynowski et al. 2011; Al Ali et al. 2017). The larger propor- tion of PAHs with a high molecular weight may be due to their common source in vehicle emissions (Hassanien and Abdel-Latif 2008; Lorenzi et al. 2011; Wang et al. 2011). In DD, combustion PAHs, the sum of Flt, Pyr, BaA, Chr, B(b + k)F, and BaP (Rogge et al. 1993a; Keshavarzi et al. 2018) constitute a notable contribution of the total, in the range of 986.60- 1069.42 µg kg^{-1} dw, with a mean value of 740.04 µg kg^{-1} dw. DRs for PAHs are shown in Fig. 3b, which indicates that the source for most samples was petroleum combustion.

According to transportation statistics reports, the number of passengers who traveled to Mashhad in 2018 was more than 25 million, 32% of which traveled to this city in the summer. As a consequence, summer brings a rise in the number of passengers on buses, trains, and flights. According to meteorological statistics for Mashhad for 2018, the months of June

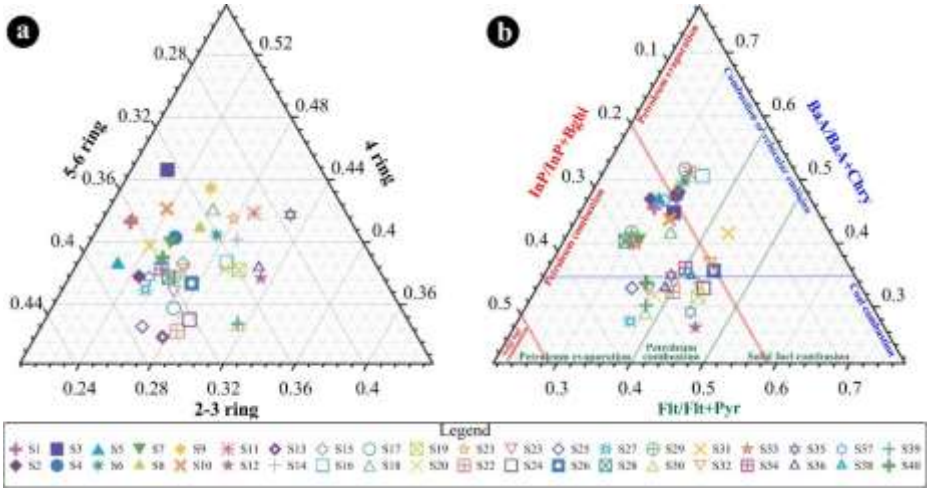

Fig. 3 **(a)** Triangular diagram of percentage concentration for the PAHs in Mashhad deposited dust samples, **(b)** Diagnostic ratios based on PAH parents and isomers for source identification in Mashhad deposited dust samples

(25.5 °C), July (30.17 °C) and August (28.7 °C) had the highest temperature and the minimum rainfall of the year. In these months of the year, lack of rainfall and high temperatures cause a decrease in soil moisture, resulting in the suspension of soil particles due to wind and a rise in dust and particles (Abbasi and Keshavarzi 2019). In addition, according to Mashhad annual report on environmental pollutants for 2018, the first half of the year saw higher levels of PM_{10} (https://epmc.mashhad.ir//parameters/mashhad/modules/cdk/upload/content/file_manager/11159/mashhad%20annual%20report%201397.pdf). Higher concentrations of suspended particles were found in the studied stations during the spring and summer, which is consistent with the findings of surface dust in the current study.

Two factors were defined as reflecting different source categories or physicochemical behavior in the results of PCA analysis, as shown in Fig. SM2 and Table 3: 4–5 ring compounds, including Ant, Flt, Pyr, BaA, BbF, BkF, InP, DahA and BghiP. BghiP dominated in the first factor (with 49.20% of the total variance) (Rogge et al. 1993a; Mostafa et al. 2009; Boonyatumanond et al. 2007) and Flt and Pyr, which are associated with diesel emis- sions (Mostafa et al. 2009). DahA, which is associated with fossil fuel combustion (Rogge et al. 1993a; Boonyatumanond et al. 2007) and InP specifically associated with gasoline emissions (Mostafa et al. 2009). In summary, Factor 1 was assigned to vehicular traffic contamination.

Nap, Acy, Ace, Chr, Phe and BaP had high loadings of Factor 2 (38.55% of the total variance). Low molecular weight compounds such as Nap, Acy and Ace are produced by burning straw and firewood (Dong and Lee 2009; Jiang et al. 2014). BaP emissions can be specifically related to biomass combustion (Park et al. 2002; Lin et al. 2010), napthalene emissions are associated with petroleum application due to its direct relevance with incomplete combustion sources (Jiang et al. 2014; Moeinaddini et al. 2014a), and Chr emissions are associated with natural gas combustion (Harrison et al. 1996). Factor 2 represents wood,

Table 3 The results of principal component analysis (PCA) for PAHs

	PAH factor	
	1	**2**
Nap	0.49	***0.67***
Acy	0.14	***0.84***
Ace	0.28	***0.84***
Flo	0.62	0.38
Phe	0.48	***0.63***
Ant	***0.77***	0.06
Flt	***0.95***	0.10
Pyr	***0.89***	0.30
BaA	***0.87***	0.11
Chr	-0.10	***0.80***
BbF	***0.54***	0.50
BkF	***0.57***	0.47
BaP	0.24	***0.76***
InP	***0.58***	0.27
DahA	***0.62***	0.12
BghiP	***0.74***	0.48

[a] Values in bold/italics are for factor loading values> 0.5 and indicate important factors for each component

biomass, and incomplete combustion-related sources, as well as natural gas combustion, based on the high loading values of these PAHs (Fang et al. 2004).

3.4 Risk Assessment

The compounds that contributed the most to carcinogenic risk, as shown in Table 4, are BaP and DahA, which accounted for 24.73% and 47.91% of the total BaP_{TEQ}, respec- tively. In most monitored systems, an ILCR of $10^{-6} – 10^{-4}$ indicates a potential risk, as the ILCR < 10^{-6} implies relative safety and the ILCR > 10^{-4} presents high risk (Guo et al. 2003; Gope et al. 2018). The carcinogenic risk from ingestion and dermal touch was around 10^{-7} for adults and infants, while the risk from inhalation was between 10^{-11} to 10^{-12}. In a comparison of exposure methods (ingestion and dermal contact; Wu et al. 2018), dermal contact was identified as the main exposure pathway to cancer risk, and the latter exposure risk was almost negligible.

In combination with non-dietary use of PAHs in DD from homes in Ottawa, Canada, Maertens et al. (2008) estimated higher surplus lifetime cancer risks for preschool children, ranging from 10^{-6} and 10^{-4}. So, in the current study, the total carcinogenic risk for children (8.45×10^{-12}) indicated no risk, while for adults (9.80×10^{-7}) was the nearest to the initial admissible risk of 10^{-6}. Despite the relatively low risks involved, if the influx of visitors grows without any control over traffic movements, and with DRs suggesting sources of PAHs from vehicular traffic, these risks are likely to increase unless urgent action is taken.

3.5 Relationships between Variables

The aim of cluster analysis was to discover the relationship between variables (stations, *n*-alkanes, PAHs, hopanes, steranes and some diagnostic ratios). Standardization was done prior to clustering, due to the distinctive scales of the variables. Figure 4 shows the heat map (DHCA) results.

These clusters are identified by inspecting the correlation matrix of the parameters, and the parameters generally in each cluster are strongly correlated. The colors describe the relationship between the parameters. The vertical dendogram illustrates how sampling locations are clustered based on different variables. The horizontal dendogram shows how the various variables are grouped together based on their similarities (Fig. 4). DHCA separates the sampling sites into two clusters in the horizontal dendogram. The findings suggest that the distribution of ∑16PAHs, ∑20*n*-alkanes, ∑8hopanes and ∑6steranes varies by sampling

Table 4 The incremental lifetime cancer risk (ILCR) for children and adults in deposited dust of Mashhad, Iran

Exposure pathways	Child				Adult			
	ILCR ingestion	ILCR inhalation	ILCR Dermal	Cancer risk	ILCR ingestion	ILCR inhalation	ILCR Dermal	Cancer risk
Min	2E-07	2.562E-07	1.55145E-11	4.96787E-12	3.55339E-07	3.19389E-07	5.55391E-07	5.75607E-07
Max	4.862E-07	6.228E-07	3.77096E-11	1.20749E-11	8.63688E-07	7.76308E-07	1.34994E-06	1.39907E-06
Mean	3.405E-07	4.361E-07	2.64061E-11	8.45544E-12	6.04795E-07	5.43608E-07	9.45288E-07	9.79698E-07

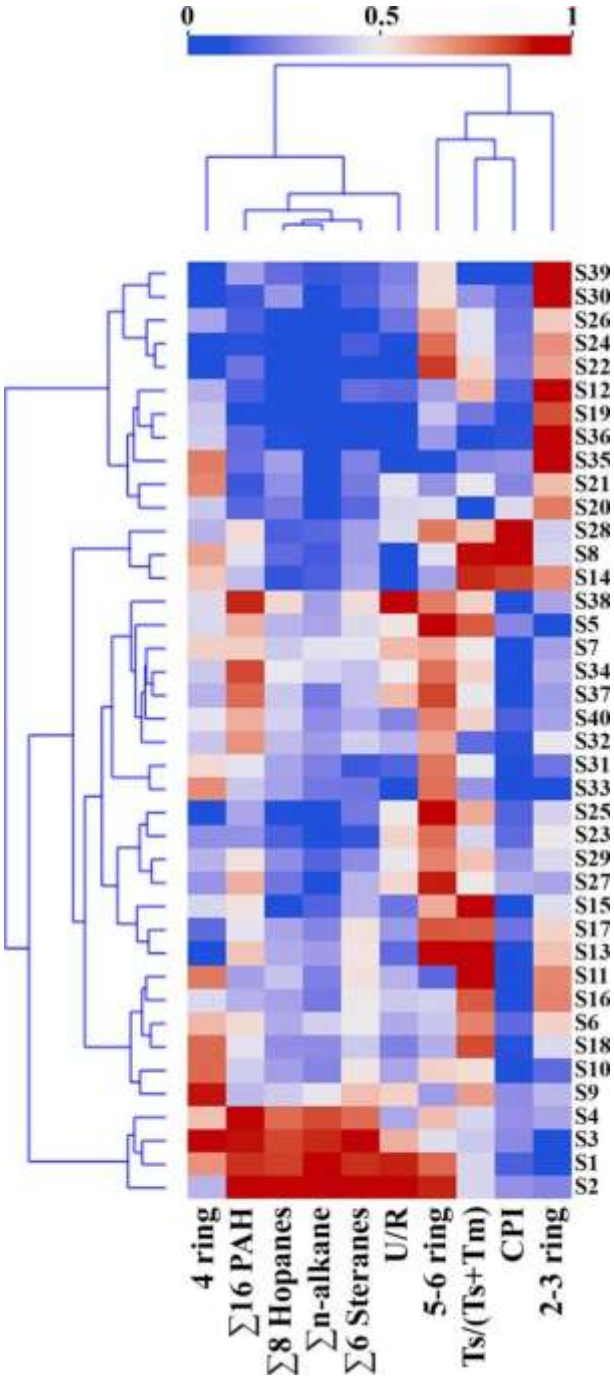

Fig. 4 Heat map (DHCA analysis) indicating the relationship between variables (stations, ∑16 PAHs, ∑20 *n*-alkanes, ∑8 hopanes, ∑6 steranes) in deposited dust samples of Mashhad, Iran

site in the city, with the colors implying the relationship between parameters and sampling stations. In terms of vertical dendrogram, DHCA groups sampling points into 2 clusters.

Cluster 1 is made up of high-traffic sampling points and sampling points near highways. Cluster 2 is composed of sampling points in close proximity to residential areas. According to the results of DHCA and the impact of urban traffic on the clustering of sampling points, it is fair to believe that the aromatic and aliphatic hydrocarbon emissions in this area could have an adverse effect on tourism, socioeconomic conditions, and air quality in this city.

4 Conclusions

In deposited dust (DD) from Mashhad, Iran, high levels of aromatic and aliphatic hydrocarbons (PAHs, *n*-alkanes, hopane and steranes) were found near the heavily trafficked city center and bus terminal. The majority of *n*-alkanes in urban DD originate from vehicular emissions, with minor contribution from higher plant waxes. The low values of the carbon preference index (CPI ~1) and the high values of unresolved components to resolved components in gas chromatograms (U:R) support this finding. The presence of pristane, phytane, hopanes, and steranes in DD, and even unresolved complex mixtures (UCM), indicates that it has been polluted by petroleum residues originated from vehicular emissions. The molecular distribution of hopanes and steranes is very similar to that of vehicular exhaust. The urban historical structure in Mashhad also affects the occurrence and distribution of PAHs in DD. In contrast to residential areas, the oldest urban areas (near the holy shrine) have more polluted dust, around three times the concentrations of some PAHs. The results of diagnostic ratios (DRs) and PCA analysis show that the major compounds contained in the DD were high molecular weight PAHs, implying a combustion origin.

Based on the results of this study, diesel and gasoline-powered vehicles are responsible for a significant proportion of the hydrocarbon pollution in Mashhad; technological monitoring and improvements in the efficiency of diesel and gasoline vehicles will help to minimize these emissions. The findings of this study are applicable to similar urban areas around the world, principally those with known heritage sites or tourist influxes. It also operates as a scientific foundation for relevant authorities and policy-makers to formulate and implement policy and air pollution mitigation measures to regulate and monitor traffic-related fine aerosol emissions, protecting the environment and public health. At last, it should be noted that total cancer risk for both children (8.45×10^{-12}) and adults (9.80×10^{-7}) in this research is in the range of virtual safety, making the risk of cancer for teens and adults who study and work in these buildings insignificant.

References

Abbasi S, Keshavarzi B (2019) Source identification of total petroleum hydrocarbons and polycyclic aromatic hydrocarbons in PM10 and street dust of a hot spot for petrochemical production: Asaluyeh County, Iran. Sustainable Cities and Society 45:214–230

Abbasnejad B, Keshavarzi B, Mohammadi Z, Moore F, Abbasnejad A (2019) Characteristics, distribution, source apportionment, and potential health risk assessment of polycyclic aromatic hydrocarbons in urban street dust of Kerman metropolis, Iran. Int J Environ Health Res 29:668–685

Al-Rajhi M, Seaward M, Al-Aamer A (1996) Metal levels in indoor and outdoor dust in Riyadh, Saudi Arabia. Environ Int 22:315–324

Al Ali S, Debade X, Chebbo G, Béchet B, Bonhomme C (2017) Contribution of atmospheric dry deposition to stormwater loads for PAHs and trace metals in a small and highly trafficked urban road catchment. Environ Sci Pollut Res 24:26497–26512

Alves C, Evtyugina M, Vicente A, Vicente E, Nunes T, Silva P, Duarte M, Pio C, Amato F, Querol X (2018) Chemical profiling of PM10 from urban road dust. Sci Total Environ 634:41–51

Alves CA, Vicente AM, Rocha S, Vasconcellos P (2017) Hopanoid hydrocarbons in PM 10 from road tunnels in São Paulo, Brazil. Air Quality, Atmosphere and Health 10: 799–807

Andreou G, Alexiou S, Loupa G, Rapsomanikis S (2008) Identification, abundance and origin of aliphatic hydrocarbons in the fine atmospheric particulate matter of Athens. Greece Water Air and Soil Pollution: Focus 8:99–106

Azari KA, Arintono S (2012) Congestion pricing scheme in Mashhad, Iran: overview description, impacts and behavioural responsiveness. World Appl Sci J 20:1484–1492

Azimi A, Bakhtiari AR, Tauler R (2018) Chemometrics analysis of petroleum hydrocarbons sources in the street dust, runoff and sediment of urban rivers in Anzali port-South of Caspian Sea. Environ Pollut 243:374–382

Azimi A, Bakhtiari AR, Tauler R (2020) Polycyclic aromatic hydrocarbon source fingerprints in the environmental samples of Anzali—South of Caspian Sea. Environ Sci Pollut Res 27:32719–32731

Bahry PS, Zakaria MP, Bin Abdullah AM, Abdullah DK, Sakari M, Chandru K, Shahbazi A (2009) Forensic characterization of polycyclic aromatic hydrocarbons and hopanes in aerosols from peninsular Malaysia. Environ Forensics 10:240–252

Bakhtiari AR, Zakaria MP, Yaziz MI, Lajis MNH, Bi X (2009) Polycyclic aromatic hydrocarbons and n-alkanes in suspended particulate matter and sediments from the Langat River, Peninsular Malaysia. Environ Asia 2:1–10

Bakhtiari AR, Zakaria MP, Yaziz MI, Lajis MNH, Bi X (2011) Variations and origins of aliphatic hydrocarbons in sediment cores from Chini Lake in Peninsular Malaysia. Environ Forensics 12:79–91

Bian Q, Alharbi B, Collett J Jr, Kreidenweis S, Pasha MJ (2016) Measurements and source apportionment of particle-associated polycyclic aromatic hydrocarbons in ambient air in Riyadh, Saudi Arabia. Atmos Environ 137:186–198

Boonyatumanond R, Murakami M, Wattayakorn G, Togo A, Takada H (2007) Sources of polycyclic aromatic hydrocarbons (PAHs) in street dust in a tropical Asian mega-city, Bangkok, Thailand. Science of the Total Environment 384: 420–432

Chattopadhyay G, Lin KC-P, Feitz AJ (2003) Household dust metal levels in the Sydney metropolitan area. Environ Res 93:301–307

Davoudi M, Esmaili-Sari A, Bahramifar N, Moeinaddini MJES (2021) Spatio-temporal variation and risk assessment of polycyclic aromatic hydrocarbons (PAHs) in surface dust of Qom metropolis, Iran. Environ Sci Pollut Res 28:9276–9289

Delgado-Saborit JM, Stark C, Harrison RM (2011) Carcinogenic potential, levels and sources of polycyclic aromatic hydrocarbon mixtures in indoor and outdoor environments and their implications for air quality standards. Environ Int 37:383–392

Dong TT, Lee B-K (2009) Characteristics, toxicity, and source apportionment of polycylic aromatic hydrocarbons (PAHs) in road dust of Ulsan, Korea. Chemosphere 74:1245–1253
Du W, Yun X, Chen Y, Zhong Q, Wang W, Wang L, Qi M, Shen G, Tao S (2020) PAHs emissions from residential biomass burning in real-world cooking stoves in rural China. Environ Pollut 267:115592
Duan F, He K, Liu X (2010) Characteristics and source identification of fine particulate n-alkanes in Beijing, China. J Environ Sci 22:998–1005
El Haddad I, Marchand N, Dron J, Temime-Roussel B, Quivet E, Wortham H, Jaffrezo JL, Baduel C, Voisin D, Besombes JL (2009) Comprehensive primary particulate organic characterization of vehicular exhaust emissions in France. Atmos Environ 43:6190–6198
Fang G-C, Chang C-N, Wu Y-S, Fu PP-C, Yang I-L, Chen M-H (2004) Characterization, identification of ambient air and road dust polycyclic aromatic hydrocarbons in central Taiwan, Taichung. Sci Total Environ 327:135–146
Ghanavati N, Nazarpour A, Watts MJ (2019) Status, source, ecological and health risk assessment of toxic metals and polycyclic aromatic hydrocarbons (PAHs) in street dust of Abadan. Iran Catena 177:246–259
pe M, Masto RE, George J, Balachandran S (2018) Exposure and cancer risk assessment of polycyclic aromatic hydrocarbons (PAHs) in the street dust of Asansol city, India. Sustainable Cities and Society 38:616–626
Guo H, Lee S, Ho K, Wang X, Zou S (2003) Particle-associated polycyclic aromatic hydrocarbons in urban air of Hong Kong. Atmos Environ 37:5307–5317
Han F, Cao J, Peng L, Bai H, Hu D, Mu L, Liu X (2015) Characteristics of hopanoid hydrocarbons in ambient PM 10 and motor vehicle emissions and coal ash in Taiyuan, China. Environ Geochem Health 37:813–829
Harrison RM, Smith D, Luhana L (1996) Source apportionment of atmospheric polycyclic aromatic hydrocarbons collected from an urban location in Birmingham, UK. Environ Sci Technol 30:825–832
Hassanien MA, Abdel-Latif NM (2008) Polycyclic aromatic hydrocarbons in road dust over Greater Cairo, Egypt. J Hazard Mater 151:247–254
He LY, Hu M, Huang XF, Zhang YH, Yu BD, Liu DQ (2006) Chemical characterization of fine particles from on-road vehicles in the Wutong tunnel in Shenzhen, China. Chemosphere 62:1565–1573
Holopainen R, Tuomainen M, Asikainen V, Pasanen P, Sateri J, Seppanen O (2002) The effect of cleanliness control during installation work on the amount of accumulated dust in ducts of new HVAC installations. Indoor Air 12:191–197
Hussain K, Rahman M, Prakash A, Hoque RR (2015) Street dust bound PAHs, carbon and heavy metals in Guwahati city–Seasonality, toxicity and sources. Sustainable Cities and Society 19:17–25
Jafarabadi AR, Bakhtiari AR, Hedouin L, Toosi AS, Cappello T (2018) Spatio-temporal variability, distribution and sources of n-alkanes and polycyclic aromatic hydrocarbons in reef surface sediments of Kharg and Lark coral reefs, Persian Gulf, Iran. Ecotoxicol Environ Saf 163:307–322
Jafarabadi AR, Dashtbozorg M, Bakhtiari AR, Maisano M, Cappello T (2019) Geochemical imprints of occurrence, vertical distribution and sources of aliphatic hydrocarbons, aliphatic ketones, hopanes and steranes in sediment cores from ten Iranian Coral Islands, Persian Gulf. Mar Pollut Bull 144:287–298
Javed W, Iakovides M, Garaga R, Stephanou EG, Kota SH, Ying Q, Wolfson JM, Koutrakis P, Guo B (2019) Source apportionment of organic pollutants in fine and coarse atmospheric particles in Doha, Qatar. J Air Waste Manag Assoc 69:1277–1292
Jiang Y, Hu X, Yves UJ, Zhan H, Wu Y (2014) Status, source and health risk assessment of polycyclic aromatic hydrocarbons in street dust of an industrial city, NW China. Ecotoxicol Environ Saf 106:11–18
Jordanova D, Jordanova N, Lanos P, Petrov P, Tsacheva T (2012) Magnetism of outdoor and indoor settled dust and its utilization as a tool for revealing the effect of elevated particulate air pollution on cardiovascular mortality. Geochemistry, Geophysics, Geosystems 13:1–27
Keshavarzi B, Abbasi S, Moore F, Mehravar S, Sorooshian A, Soltani N, Najmeddin A (2018) Contamination level, source identification and risk assessment of potentially toxic elements (PTEs) and polycyclic aromatic hydrocarbons (PAHs) in street dust of an important commercial center in Iran. Environ Manage 62:803–818
Keshavarzi B, Abbasi HS, Moore F, Delshab H, Soltani N (2020) Polycyclic aromatic hydrocarbons in street dust of Bushehr City, Iran: status, source, and human health risk assessment. Polycycl Aromat Compd 40:61–75
Khedidji S, Ladji R, Yassaa N (2013) A wintertime study of polycyclic aromatic hydrocarbons (PAHs) in indoor and outdoor air in a big student residence in Algiers, Algeria. Environ Sci Pollut Res 20:4906–4919
Konstantinova E, Minkina T, Sushkova S, Antonenko E, Konstantinov A (2020) Levels, sources, and toxicity assessment of polycyclic aromatic hydrocarbons in urban topsoils of an intensively developing Western Siberian city. Environ Geochem Health 42:325–341

Kozliak EI, Paca J (2012) Journal of Environmental Science and Health, Part A. Toxic/hazardous Substances and Environmental Engineering: Foreword 47(7): 919. DOI: https://doi.org/10.1080/10934529.2012.667287
Kramer SJ, Alvarez C, Barkley AE, Colarco PR, Custals L, Delgadillo R, Gaston CJ, Govindaraju R, Zuidema P (2020) Apparent dust size discrepancy in aerosol reanalysis in north African dust after long-range transport. Atmos Chem Phys 20:10047–10062
Lin L, Lee ML, Eatough DJ (2010) Review of recent advances in detection of organic markers in fine particulate matter and their use for source apportionment. J Air Waste Manag Assoc 60:3–25
Liu J, Man R, Ma S, Li J, Wu Q, Peng J (2015) Atmospheric levels and health risk of polycyclic aromatic hydrocarbons (PAHs) bound to PM2. 5 in Guangzhou, China. Mar Pollut Bull 100:134–143
Liu R, He R, Cui X, Ma LQ (2018) Impact of particle size on distribution, bioaccessibility, and cytotoxicity of polycyclic aromatic hydrocarbons in indoor dust. J Hazard Mater 357:341–347
Liu Y, Chen L, Huang Q-h, Li W-y, Tang Y-j, Zhao J-f (2009) Source apportionment of polycyclic aromatic hydrocarbons (PAHs) in surface sediments of the Huangpu River, Shanghai, China. Sci Total Environ 407:2931–2938
Lorenzi D, Entwistle JA, Cave M, Dean JR (2011) Determination of polycyclic aromatic hydrocarbons in urban street dust: implications for human health. Chemosphere 83:970–977
Ma Y, Liu A, Egodawatta P, McGree J, Goonetilleke A (2017) Quantitative assessment of human health risk posed by polycyclic aromatic hydrocarbons in urban road dust. Sci Total Environ 575:895–904
Maertens RM, Bailey J, White PA (2004) The mutagenic hazards of settled house dust: a review. Mutat Research/Reviews Mutat Res 567:401–425
Malcolm H, Dobson S (1994) The calculation of a Regulatory Assessment Level (RAL) for atmospheric PAHs based on relative potencies. first draft
Martuzevicius D, Kliucininkas L, Prasauskas T, Krugly E, Kauneliene V, Strandberg B (2011) Resuspension of particulate matter and PAHs from street dust. Atmos Environ 45:310–317
Marynowski L, Kurkiewicz S, Rakociński M, Simoneit BR (2011) Effects of weathering on organic matter: I. Changes in molecular composition of extractable organic compounds caused by paleoweathering of a Lower Carboniferous (Tournaisian) marine black shale. Chem Geol 285:144–156
Mihankhah T, Saeedi M, Karbassi AJE (2020) safety e Contamination and cancer risk assessment of polycyclic aromatic hydrocarbons (PAHs) in urban dust from different land-uses in the most populated city of Iran. Ecotoxicology and Environemenral Safety 187: 109838
Moeinaddini M, Sari AE, Bakhtiari AR, Chan AY-C, Taghavi SM, Connell D, Hawker D (2014a) Sources and Health Risk of Organic Compounds in Respirable Particles in Tehran, Iran. Polycycl Aromat Compd 34:469–492
Moeinaddini M, Sari AE, Chan AY-C, Taghavi SM, Hawker D, Connell D (2014b) Source apportionment of PAHs and n-alkanes in respirable particles in Tehran, Iran by wind sector and vertical profile. Environ Sci Pollut Res 21:7757–7772
Mon EE, Phay N, Agusa T, Bach LT, Yeh H-M, Huang C-H, Nakata H (2020) Polycyclic Aromatic Hydrocarbons (PAHs) in Road Dust Collected from Myanmar, Japan, Taiwan, and Vietnam. Arch Environ Contam Toxicol 78:34–45
Mostafa A, Hegazi A, El-Gayar MS, Andersson J (2009) Source characterization and the environmental impact of urban street dusts from Egypt based on hydrocarbon distributions. Fuel 88:95–104
Najmeddin A, Moore F, Keshavarzi B, Sadegh Z (2018) Pollution, source apportionment and health risk of potentially toxic elements (PTEs) and polycyclic aromatic hydrocarbons (PAHs) in urban street dust of Mashhad, the second largest city of Iran. J Geochem Explor 190:154–169
Najmeddin A, Keshavarzi B (2019) Health risk assessment and source apportionment of polycyclic aromatic hydrocarbons associated with PM 10 and road deposited dust in Ahvaz metropolis of Iran. Environ Geochem Health 41:1267–1290
Nisbet IC, Lagoy PK (1992) Toxic equivalency factors (TEFs) for polycyclic aromatic hydrocarbons (PAHs). Regul Toxicol Pharmacol 16:290–300
Nowakowski M, Rykowska I, Wolski R, Andrzejewski P (2022) Polycyclic Aromatic Hydrocarbons (PAHs) and their Derivatives (O-PAHs, N-PAHs, OH-PAHs): Determination in Suspended Particulate Matter (SPM) a Review. Environ Processes 9:1–27
Ofori SA, Cobbina SJ, Imoro A, Doke DA, Gaiser T (2021) Polycyclic Aromatic Hydrocarbon (PAH) Pollution and its Associated Human Health Risks in the Niger Delta Region of Nigeria: A Systematic Review. Environ Processes 8:455–482
Omar NYM, Abas MRB, Ketuly KA, Tahir NM (2002) Concentrations of PAHs in atmospheric particles (PM-10) and roadside soil particles collected in Kuala Lumpur, Malaysia. Atmos Environ 36:247–254

Omar NYM, Abas MRB, Rahman NA, Tahir NM, Rushdi AI, Simoneit BR (2007) Levels and distributions of organic source tracers in air and roadside dust particles of Kuala Lumpur, Malaysia. Environ Geol 52:1485–1500
Pandit G, Srivastava P, Rao AM (2001) Monitoring of indoor volatile organic compounds and polycyclic aromatic hydrocarbons arising from kerosene cooking fuel. Sci Total Environ 279:159–165
Park SS, Kim YJ, Kang CH (2002) Atmospheric polycyclic aromatic hydrocarbons in Seoul. Korea Atmospheric Environment 36:2917–2924
Pham CT, Kameda T, Toriba A, Hayakawa K (2013) Polycyclic aromatic hydrocarbons and nitropolycyclic aromatic hydrocarbons in particulates emitted by motorcycles. Environ Pllution 183:175–183
Pongpiachan S, Hattayanone M, Suttinun O, Khumsup C, Kittikoon I, Hirunyatrakul P, Cao J (2017) Assessing human exposure to PM10-bound polycyclic aromatic hydrocarbons during fireworks displays. Atmospheric Pollution Research 8:816–827
Rastegari Mehr M, Keshavarzi B, Moore F, Sacchi E, Lahijanzadeh AR, Eydivand S, Jaafarzadeh N, Naserian S, Setti M, Rostami S (2016) Contamination level and human health hazard assessment of heavy metals and polycyclic aromatic hydrocarbons (PAHs) in street dust deposited in Mahshahr, southwest of Iran. Human and Ecological Risk Assessment: An International Journal 22: 1726–1748
Ravindra K, Sokhi R, Van Grieken R (2008) Atmospheric polycyclic aromatic hydrocarbons: source attribution, emission factors and regulation. Atmos Environ 42:2895–2921
Rogge WF, Hildemann LM, Mazurek MA, Cass GR, Simoneit BR (1993a) Sources of fine organic aerosol. 2. Noncatalyst and catalyst-equipped automobiles and heavy-duty diesel trucks. Environ Sci Technol 27:636–651
Rogge WF, Mazurek MA, Hildemann LM, Cass GR, Simoneit BR (1993b) Quantification of urban organic aerosols at a molecular level: identification, abundance and seasonal variation. Atmospheric Environ Part Gen Top 27:1309–1330
Saeedi M, Li LY, Salmanzadeh M (2012) Heavy metals and polycyclic aromatic hydrocarbons: pollution and ecological risk assessment in street dust of Tehran. J Hazard Mater 227:9–17
Sajn R (2005) Using attic dust and soil for the separation of anthropogenicand geogenic elemental distributions in an old metallurgic area (Celje, Slovenia). Geochemistry: Exploration, Environment, Analysis 5: 59–67
Sanchis E, Ferrer M, Calvet S, Coscollà C, Yusà V, Cambra-López M (2014) Gaseous and particulate emission profiles during controlled rice straw burning. Atmos Environ 98:25–31
Shirneshan G, Bakhtiari AR, Memariani M (2017) Identifying the source of petroleum pollution in sediment cores of southwest of the Caspian Sea using chemical fingerprinting of aliphatic and alicyclic hydrocarbons. Mar Pollut Bull 115:383–390
Simoneit BR, Mazurek MA (1982) Organic matter of the troposphere—II. Natural background of biogenic lipid matter in aerosols over the rural western United States. Atmos Environ 16:2139–2159
Simoneit BR (1984) Organic matter of the troposphere—III. Characterization and sources of petroleum and pyrogenic residues in aerosols over the western United States. Atmos Environ 18:51–67
Simoneit BR (1985) Application of molecular marker analysis to vehicular exhaust for source reconciliations. Int J Environ Anal Chem 22:203–232
Simoneit BR (1999) A review of biomarker compounds as source indicators and tracers for air pollution. Environ Sci Pollut Res 6:159–169
Škrbić B, Đurišić-Mladenović N, Živančev J, Tadić Đ (2019) Seasonal occurrence and cancer risk assessment of polycyclic aromatic hydrocarbons in street dust from the Novi Sad city, Serbia. Sci Total Environ 647:191–203
Škrbić BD, Đurišić-Mladenović N, Tadić ĐJ, Cvejanov J (2017) Polycyclic aromatic hydrocarbons in urban soil of Novi Sad, Serbia: occurrence and cancer risk assessment. Environ Sci Pollut Res 24:16148–16159
Škrbić BD, Antić I, Živančev J, Vágvölgyi C (2021) Comprehensive characterization of PAHs profile in Serbian soils for conventional and organic production: potential sources and risk assessment. Environ Geochem Health 43:4201–4218
Soleimani Z, Goudarzi G, Sorooshian A, Marzouni MB, Maleki H (2016) Impact of Middle Eastern dust storms on indoor and outdoor composition of bioaerosol. Atmos Environ 138:135–143
Soltani N, Keshavarzi B, Moore F, Tavakol T, Lahijanzadeh AR, Jaafarzadeh N, Kermani M (2015) Ecological and human health hazards of heavy metals and polycyclic aromatic hydrocarbons (PAHs) in road dust of Isfahan metropolis, Iran. Sci Total Environ 505:712–723
Takada H, Onda T, Harada M, Ogura N (1991) Distribution and sources of polycyclic aromatic hydrocarbons (PAHs) in street dust from the Tokyo Metropolitan area. Sci Total Environ 107:45–69
Thomas CL, Jansen B, van Loon EE, Wiesenberg GL (2021) Transformation of n-alkanes from plant to soil: a review. Soil 7:785–809
Tringe SG, Zhang T, Liu X, Yu Y, Lee WH, Yap J, Yao F, Suan ST, Ing SK, Haynes M (2008) The airborne metagenome in an indoor urban environment. PLoS ONE 3:e1862

Wang W, Huang M-j, Kang Y, Wang H-s, Leung AO, Cheung KC, Wong MH (2011) Polycyclic aromatic hydrocarbons (PAHs) in urban surface dust of Guangzhou, China: Status, sources and human health risk assessment. Sci Total Environ 409:4519–4527

Wu S, Liu X, Liu M, Chen X, Liu S, Cheng L, Lin X, Li Y (2018) Sources, influencing factors and environmental indications of PAH pollution in urban soil columns of Shanghai, China. Ecol Ind 85:1170–1180

Wu Y, Shi Y, Zhang N, Wang Y, Ren Y (2021) Pollution levels, characteristics, and sources of polycyclic aromatic hydrocarbons in atmospheric particulate matter across the Hu line in China. A review. Environ Chem Lett 19:3821–3836

Yadav S, Tandon A, Attri AK (2013) Characterization of aerosol associated non-polar organic compounds using TD-GC-MS: a four year study from Delhi, India. J Hazard mMterials 252:29–44

Yang W, Cao Z, Lang Y (2021) Pollution Status of Polycyclic Aromatic Hydrocarbons (PAHs) in Northeastern China: a Review and Metanalysis. Environ Processes 8:429–454

Yunker MB, Macdonald RW, Vingarzan R, Mitchell RH, Goyette D, Sylvestre S (2002) PAHs in the Fraser River basin: a critical appraisal of PAH ratios as indicators of PAH source and composition. Org Geochem 33:489–515

Zakaria MP, Horinouchi A, Tsutsumi S, Takada H, Tanabe S, Ismail A (2000) Oil pollution in the Straits of Malacca, Malaysia: Application of molecular markers for source identification. Environ Sci Technol 34:1189–1196

Zakaria MP, Takada H, Tsutsumi S, Ohno K, Yamada J, Kouno E, Kumata H (2002) Distribution of polycyclic aromatic hydrocarbons (PAHs) in rivers and estuaries in Malaysia: a widespread input of petrogenic PAHs. Environ Sci Technol 36:1907–1918

Zhang Y, Shen Z, Sun J, Zhang L, Zhang B, Zou H, Zhang T, Ho SSH, Chang X, Xu H (2021) Parent, alkylated, oxygenated and nitrated polycyclic aromatic hydrocarbons in PM2. 5 emitted from residential biomass burning and coal combustion: A novel database of 14 heating scenarios. Environ Pollut 268:115881

Zhang Z-H, Khlystov A, Norford LK, Tan Z-K, Balasubramanian R (2017) Characterization of traffic-related ambient fine particulate matter (PM2. 5) in an Asian city: Environmental and health implications. Atmos Environ 161:132–143

Zhen XL, Liu G, Li JH, Xu H, Wu DJ (2020) PAHs in road dust of Nanjing Chemical Industry Park, China: chemical composition, sources, and risk assessment. J Environ Sci Health Part A 55:33–43

Zheng H, Kang S, Chen P, Li Q, Tripathee L, Maharjan L, Guo J, Zhang Q, Santos E (2020) Sources and spatio-temporal distribution of aerosol polycyclic aromatic hydrocarbons throughout the Tibetan Plateau. Environ Pollut 261:114144